

Elsevier Editorial System(tm) for Fish and Shellfish Immunology  
Manuscript Draft

Manuscript Number: FSIM-D-15-00289R1

Title: Which Th pathway is involved during late stage amoebic gill disease?

Article Type: Full Length Article

Keywords: amoebic gill disease; Atlantic salmon; Th pathways; cytokines; interbranchial lymphoid tissue.

Corresponding Author: Ms. Ottavia Benedicenti,

Corresponding Author's Institution: University of Aberdeen

First Author: Ottavia Benedicenti

Order of Authors: Ottavia Benedicenti; Catherine Collins, PhD; Tiehui Wang, PhD; Una McCarthy, PhD; Christopher J Secombes

Abstract: Amoebic gill disease (AGD) is an emerging disease in North European Atlantic salmon (*Salmo salar* Linnaeus 1758) aquaculture caused by the amoeba *Paramoeba perurans*. The host immune response to AGD infection is still not well understood despite past attempts to investigate host-pathogen interactions. With the significant increase in our knowledge of cytokine genes potentially involved in Th responses in recent years, we examined their involvement in this disease using Atlantic salmon post-smolts sampled 3 weeks after exposure to either 500 or 5000 cells/l *P. perurans*. Gene expression analysis of cytokines potentially involved in the different Th pathways was performed on the first gill arch including the interbranchial lymphoid tissue (ILT). Th1, Th17 and Treg pathways were found to be significantly down regulated, mainly in samples from fish given the higher dose. In contrast, the Th2 pathway was found to be significantly up regulated by both infection doses. Correlation analysis of the gene expression data and the *P. perurans* load, assessed by real time RT-PCR of the 18S rRNA, was also performed. In humans, Th2 driven responses are characterized by the production of IgE, which in the majority of worm infections results in the generation of a Th2-mediated response and directs the immune system away from a Th1 inflammatory response. The present results seen during late stage AGD suggest that either an immune evasion strategy, similar to the responses driven by helminthic parasites to avoid cell-mediated killing mechanisms, or an allergic reaction caused by the parasite is occurring.

8<sup>th</sup> May, 2015

**Ms. Ottavia Benedicenti**

Scottish Fish Immunology Research Centre

University of Aberdeen

Aberdeen, Scotland, UK

Editors of Fish and Shellfish Immunology,

Prof Chris Secombes, University of Aberdeen, Aberdeen, UK

Prof Ikuo Hirono, Tokyo University of Marine Science and Technology, Tokyo, Japan

Dear Editors,

Please find attached our paper entitled “Which Th pathway is involved during late stage amoebic gill disease?” that we are submitting for publication in your journal Fish and Shellfish Immunology. We hope the referees will find it suitable for publication in this journal.

Looking forward to hearing from you in due course.

Yours sincerely,

Ottavia Benedicenti

University of Aberdeen

**Reviewer #1:** This manuscript is interesting for the immune responses to amoeba infection in Atlantic salmon. It is almost acceptable, however, there are only several minor comments to be improved.

1. "Figure legends" (Page 15) should be located after "References".

**This has been done.**

2. In Figure legends, "mean + SEM" should be "mean  $\pm$  SEM".

**The graphs show only the positive standard error and not both positive and negative standard errors, and for this reason we believe the figure legends are correct.**

3. Figure 9, the alphabets and arrows should be more clarified (making bigger).

**They have been made bigger, in terms of the letters, arrows, scale bars and the image itself.**

**Reviewer #2:** Dear authors

I find your paper important, thorough and very well written. The parasite/host interaction is of great importance and knowledge on pathways and immune evasion strategies are very valuable. You have presented your data in an orderly and statistically solid way and I only have minor comments:

1. Please write all abbreviations in full the first time you mention them.

**Corrected.**

2. Please rewrite the sentence from line 253 - 257 on page 9.

**The sentence has been changed.**

3. Remember that the latin name (*P. perurans*) should not be in italics when it is mentioned in a headline, which is in italics.

**This has been corrected in the headline 3.3.**

4. You should go through your MS and add commas to improve reading of the text.

**More been added to improve the reading of the text.**

5. You write that Treg cells produce IL-10 and TGF-beta, which inhibit immune responses. You find that the Treg pathway is downregulated, which means that immune responses are upregulated. Does this include all immune responses? And if it does can you elaborate on this? I can't see how this would fit with an immune evasion strategy.

**TGF- $\beta$  is involved in the inhibition of T cell proliferation and macrophage activation, and promotes the development of Th17 cells and tissue repair after a local immune and inflammatory reaction. IL-10 inhibits the production of IL-12, suppressing the secretion of IFN- $\gamma$  and subsequent activation of innate and adaptive cell-mediated responses. Down regulation of the Th17 pathway could be explained by the suppression of TGF-  $\beta$ 1B expression and both down regulation of TGF-  $\beta$ 1B and IL-10 could be related to an excessive inflammatory reaction at the level of the gills caused by the presence of the amoeba. Furthermore, the balance between the Th2 cells and Treg cells is important during allergic diseases. For example, during human allergic disease, effector Th2 cells produce IL-4, IL-5, IL-9, and IL-13 and these cytokines induce the production of allergen-specific IgE by B cells, development and recruitment of eosinophils, with a production of mucus. Treg cells directly or indirectly suppress effector cells of allergic inflammation, such as mast cells, basophils, and eosinophils, and contribute to remodelling in asthma and atopic dermatitis. Increased levels of IL-10 and TGF- $\beta$  produced by Treg cells can suppress IgE production and they can be important to control the allergic inflammation. A down regulation of IL-10 and TGF- $\beta$ , as seen in this study, might be a limiting factor for the development of a healthy immune response in the case of an allergic reaction to the *P. perurans* occurring during AGD. Further comment on these points has been added to the discussion.**

6. I think you should change the maximum on your Y-axis to a lower number on some of your figures (3, 4, 5, 7). That would increase the visual understanding of the data.

**The Y-axis have been lowered for figures 3, 4, 5, 6, 7, as suggested.**

7. Can you change figure 8 so that it is visually apparent that the value is higher in the high dose? (not a must)

**The Y-axis is now in the opposite orientation, starting with high Cp value from the bottom of the axis and going to a low Cp value. In this graph it is now apparent visually that the value is higher in the higher dose.**

8. Figure 9 is too small. I can't see what you want to show me.

**The figure has been made it bigger, in terms of the letters, arrows, scale bars and the image itself.**

9. It would be very interesting to look into the role of IgT.

**Indeed, and this suggestion will be taken into account for future investigations once an anti-IgT serum has been sourced.**

I wish you good luck.

**Thank you very much.**

**Reviewer #3:** This paper describes the response of a range of genes associated with the Th pathways associated with infection of *Paramoeba perurans* in Atlantic salmon. It makes a valuable contribution to knowledge on the immune response to this important pathogen. The main issues I raise relate to clarity of certain areas which would assist the reader understanding the importance of the observations.

1. Line 114 . Centrifugation should be in 'g' not rpm.

**The values have been converted to 'g' as follows.  $6000 \text{ rpm} = 2200 \text{ x g}$  based on the formula that  $G = 1.12 \times \text{radius (mm)} \times (\text{rpm}/1000)^2$**

2. Line 228. Whilst the histopathological section a valuable contribution and the use of score between 0-5 is appropriate, the criteria used to define each stage in this score would be useful.

**The histological gill score was assessed according to Adams and Nowak (2001). The number of lesions occurring dorsally, medially and ventrally in the gill filaments were noted, along with size of lesion and the degree of pathological severity and pathological changes. This has been added to the methods.**

3. Table 2. The authors correlate the amoeba load with Cp values of the genes of interest. This is a valuable contribution but relies on the use of 18rRNA as a measure of intensity of infection of amoeba. Has the authors' supportive evidence that this parameter reflects proportionally parasite load.

**Yes, a linear relationship ( $R^2=0.9995$ ) between the log of 18S rRNA copies derived from plasmid DNA containing a partial *N. perurans* 18S RNA gene and DNA extracted from increasing numbers of *N. perurans* trophozoites was demonstrated by Bridle et al. (2010). This has been added to the methods.**

4. Fig 3 Th1 pathway IFN and Fig. 6 Th2 pathway IL4, show large SEM both associated the lower trophozoites. Are there any possible causes for the large variation in the data within these categories?

**Larger variation among individuals, as seen by the standard error bars, was found mainly when using the lower infection dose, suggesting a higher variability in infection/responsiveness with the administration of a lower dose of trophozoites. This point has been added to the discussion.**

5. Fig 9. Scale bars difficult to see.

**The letters, arrows, scale bars and image itself have been made bigger.**

## Highlights

- This report describes the characterisation of T helper responses to AGD;
- Gene expression of cytokines have been screened in the ILT of Atlantic salmon;
- Cytokines related to Th1, Th17 and Treg pathways were found down-regulated;
- Expression analysis revealed a high expression of IL-4/13A and IL-4/13B1;
- A mechanism of immune evasion or allergic response might be elicited.

1                   **Which Th pathway is involved during late stage amoebic gill disease?**

2

3                   **Ottavia Benedicenti <sup>\*a,b</sup>, Catherine Collins <sup>b</sup>, Tiehui Wang <sup>a</sup>, Una McCarthy <sup>b</sup>,**  
4   **Christopher J. Secombes <sup>\*a</sup>**

5

6   <sup>a</sup> Scottish Fish Immunology Research Centre, Institute of Biological and Environmental  
7   Sciences, University of Aberdeen, Tillydrone Avenue, Aberdeen AB24 2TZ, UK

8   <sup>b</sup> Marine Scotland Science Marine Laboratory, 375 Victoria Rd, Aberdeen AB11 9DB, UK

9

10

11   \*Corresponding authors:

12                   Ottavia Benedicenti / Chris Secombes  
13                   Scottish Fish Immunology Research Centre,  
14                   Institute of Biological and Environmental Sciences,  
15                   University of Aberdeen,  
16                   Tillydrone Avenue,  
17                   Aberdeen AB24 2TZ, UK  
18                   E-mail: r01ob13@abdn.ac.uk / c.secombes@abdn.ac.uk

19

20 **Abstract**

21 Amoebic gill disease (AGD) is an emerging disease in North European Atlantic salmon  
22 (*Salmo salar* Linnaeus 1758) aquaculture caused by the amoeba *Paramoeba perurans*. The  
23 host immune response to AGD infection is still not well understood despite past attempts to  
24 investigate host-pathogen interactions. With the significant increase in our knowledge of  
25 cytokine genes potentially involved in Th responses in recent years, we examined their  
26 involvement in this disease using Atlantic salmon post-smolts sampled 3 weeks after  
27 exposure to either 500 or 5000 cells/l *P. perurans*. Gene expression analysis of cytokines  
28 potentially involved in the different Th pathways was performed on the first gill arch  
29 including the interbranchial lymphoid tissue (ILT). Th1, Th17 and Treg pathways were found  
30 to be significantly down regulated, mainly in samples from fish given the higher dose. In  
31 contrast, the Th2 pathway was found to be significantly up regulated by both infection doses.  
32 Correlation analysis of the gene expression data and the *P. perurans* load, assessed by real  
33 time RT-PCR of the 18S rRNA, was also performed. In humans, Th2 driven responses are  
34 characterized by the production of IgE, which in the majority of worm infections results in  
35 the generation of a Th2-mediated response and directs the immune system away from a Th1  
36 inflammatory response. The present results seen during late stage AGD suggest that either an  
37 immune evasion strategy, similar to the responses driven by helminthic parasites to avoid  
38 cell-mediated killing mechanisms, or an allergic reaction caused by the parasite is occurring.

39

40 **Keywords:** amoebic gill disease, Atlantic salmon, Th pathways, cytokines, interbranchial  
41 lymphoid tissue

42

## 43 1 Introduction

44 Amoebic gill disease (AGD) is an ectoparasitic infection that affects marine fish species  
45 farmed in sea net cages [1]. The causative agent of this disease in Atlantic salmon (*Salmo*  
46 *salar* Linnaeus 1758) is *Neoparamoeba perurans* [2], an amphizoic amoeba that has  
47 successfully fulfilled the Koch's postulates [2, 3]. Recently, nuclear small subunit (SSU)  
48 rDNA phylogenetic analysis has shown that the genera *Neoparamoeba* and *Paramoeba* are  
49 phylogenetically inseparable and, therefore, *Neoparamoeba* can be used as a junior synonym  
50 of *Paramoeba* [4]. AGD has been reported from numerous countries worldwide: South  
51 Eastern Australia (Tasmania), Ireland, Japan, New Zealand, Portugal, Norway, USA, Chile,  
52 South Africa [5-11] and, since 2011, AGD has been an issue for Scottish Atlantic salmon  
53 farms, mainly in summer periods.

54 The host immune response to AGD infection in Atlantic salmon is still not well understood  
55 despite past attempts to investigate host-pathogen interactions. Early studies on  
56 transcriptional responses to AGD have shown no differences in the gill tissue expression of  
57 tumour necrosis factor (TNF)- $\alpha$ 1, TNF- $\alpha$ 2, interleukin (IL)-1 $\beta$ , inducible nitric oxide  
58 synthase (iNOS), and interferon (IFN)- $\gamma$  mRNAs compared to tissue from healthy fish, during  
59 the early onset of the disease in Atlantic salmon [12]. With the progression of the disease, IL-  
60 1 $\beta$  mRNA level was found to be up regulated and lesion-restricted in numerous studies [1,  
61 12-14]. Gene expression profiling using a 16K salmonid microarray has also been performed  
62 [15, 16]. In AGD-affected tissue, significant, coordinated down regulation of the major  
63 histocompatibility complex (MHC) class I (MHC-I) pathway-related genes occurred during  
64 the later stages of infection and appeared to be mediated by down regulation of interferon  
65 regulatory factor (IRF)-1, independent of type I interferon, IFN- $\gamma$  and IRF-2 expression [16].  
66 However, anterior gradient- (AG)-2, involved in inhibiting the tumour suppressor protein p53  
67 and required for mucin (MUC) 2 post-transcriptional synthesis and secretion, was up  
68 regulated in AGD-affected gill tissue, while p53 tumour suppressor protein mRNA was  
69 concurrently down regulated in AGD lesions, suggesting a role for AG-2 and p53 in AGD  
70 pathogenesis [17]. MHC class II<sup>+</sup> cells, considered to be antigen-presenting cells and B cells,  
71 were found within gill lesions by immunohistochemistry and it was shown that these cells  
72 exhibited variable levels of expression [17].

73 A recent study showed that mRNA expression level of pro-inflammatory cytokines (IL-1 $\beta$ ,  
74 TNF- $\alpha$ ), cellular markers of cell-mediated immunity (T cell receptor (TCR)- $\alpha$  chain, cluster  
75 of differentiation (CD) 4, CD8, MHC-I, MHC-II $\alpha$ ), and antibody-mediated immunity (IgM,

76 IgT) is correlated with a classical inflammatory response in the gills of AGD-affected  
77 Atlantic salmon at 10 days post-infection [1]. Moreover, in the same study, it was found that  
78 mRNA expression levels of these genes within gill lesions were different to the mRNA  
79 expression levels of the same genes in parts of the gill without lesions during AGD,  
80 suggesting that there are differences in the transcriptional response to AGD between areas of  
81 the gill with lesions and without lesions.

82 In 2008, a novel lymphoid tissue called the interbranchial lymphoid tissue (ILT) was  
83 discovered in the gills of salmonids and the ILT together with leucocytes in the gill filaments  
84 constitute the gill associated lymphoid tissue (GIALT) [18-20]. This novel lymphoid tissue is  
85 located at the base of the caudal edge of the interbranchial septum between the gill filaments  
86 [18] and is visible as a greyish structure by the naked eye [19]. The ILT consists largely of T-  
87 cells embedded in a meshwork of epithelial cells [19] and a few B-cells [21]. Abundant MHC  
88 class II<sup>+</sup> cells are also detectable in the epithelium on the caudal rim of the interbranchial  
89 septum and in the epithelium covering the gill filaments [18]. Functional investigations of the  
90 ILT have been performed in fish infected with infectious salmon anaemia (ISA) virus and *P.*  
91 *perurans* [21-23]. In ISA virus infected fish, there is a small delayed increase in IgT  
92 transcripts [21] and a decrease in size of the ILT compared with healthy fish [22]. Fish  
93 affected by AGD show an increased length of the ILT 28 days post exposure in the dorsal  
94 area of the gill arch, with a peak of lymphocyte density 7 days post exposure [23].

95 Further investigation of the T and B cell responses in the ILT is needed to clarify the function  
96 of this novel lymphoid tissue during AGD infection in Atlantic salmon. With the increasing  
97 number of cytokine genes that are now known, many of which may have a role in adaptive  
98 immune responses, the aim of this study was to perform an analysis of T helper (Th) type  
99 responses to AGD. For this purpose, gene expression profiles of signature cytokines produced  
100 by Th subsets (Th1, Th2, Th17, regulatory T cells - Treg) were screened in the ILT of  
101 Atlantic salmon infected with amoeba at two different concentrations (500 and 5000 cells/l),  
102 to determine their potential role in host defences against this parasite.

## 103 **2 Materials and Methods**

### 104 *2.1 Amoeba culture*

105 The amoebae were cultivated at 15 °C in small petri dishes containing a 5 ml underlay of  
106 malt yeast agar (MYA) (0.05 g malt extract, 0.05 g yeast extract, 10.00 g bacteriological agar,  
107 500 ml of 35 ppt filtered seawater), with approximately 7 ml overlay of 35 ppt filtered

108 sterilized seawater. Stericup® Filter Units (© EMD Millipore Corporation, Billerica, MA,  
109 USA, 2014) with a 0.22 µm pore size were used to filter the seawater coming from the North  
110 Sea (ca. 35 ppt salinity). Cultures were maintained in a non-axenic environment containing  
111 different bacterial strains isolated with amoebae from gills during culture establishment.

## 112 2.2 *In vivo challenge and sampling of ILT*

113 Amoebae were cultivated to reach a concentration of 500 cells/l and 5000 cells/l for the *in*  
114 *vivo* challenge. The neutral red (NR)-assay was used to determine cell viability. Briefly, 0.35  
115 µl of neutral red (Sigma-Aldrich, Germany) was added to a 100 µl aliquot of amoeba  
116 cultures. After 30 min to allow NR uptake, amoebae were centrifuged at 2200 x g for 10 min,  
117 the supernatant was removed and amoebae resuspended in 100 µl of sterilized seawater (35  
118 ppt). Counts were performed in triplicate in 96-well plates.

119 The experiment was designed to establish an AGD challenge with a type I error of 5%  
120 assuming a success rate of 70% (power analysis). Atlantic salmon were taken through  
121 smoltification in aquarium facilities at the Marine Scotland Science Marine Laboratory in  
122 Aberdeen, UK. Fish were held at 12 °C in full-strength seawater (ca. 35 ppt) and fed daily to  
123 1% body weight using the Skretting Atlantic Smolt diet. Two groups of 5 fish (ca. 400 g)  
124 were exposed to 500 cells/l and 5000 cells/l in a total volume of 120 l of seawater (ca. 33 - 35  
125 ppt) and held in this static volume, with aeration, for 4 h. The same procedure was applied for  
126 a negative control where 5 fish were exposed to the medium used for amoeba culture, which  
127 was filtered with a 3.0 µm pore size Cyclopore™ Track Etched Membrane (GE Healthcare,  
128 Whatman, UK), in order to separate out the amoebae but retain the culture bacteria. No signs  
129 of distress were observed in fish during this period. After 4 h, the water volume was  
130 increased to 350 l and exchanged in a flow through system at a rate of 3 l/min. Fish were fed  
131 daily to satiation. At 3 weeks post-exposure, fish were anaesthetised with 0.3 g/l of ethyl 3-  
132 aminobenzoate methanesulfonate (MS-222, Sigma-Aldrich, Germany) and killed. Tissue  
133 samples from the first gill arch were collected, primarily to include the interbranchial  
134 lymphoid tissue (ILT) avoiding the gill arch and the end of the gill filaments (Fig. 1). Gill  
135 samples were stored in RNAlater (RNAlater® Stabilization Solution, Ambion®) at - 80 °C  
136 for gene expression and *P. perurans* load analyses.

137 For histological analysis and assessment of the pathology associated with AGD, samples  
138 from the first gill arch were fixed in 10% buffered neutral formalin solution for a minimum of  
139 24 h, washed in 100% ethanol (EtOH), and then stored in 70% EtOH until processing.  
140 Samples were then washed three times in 100% EtOH, in xylene (3 dips) and embedded in

141 paraffin wax. Sections (3  $\mu\text{m}$ ) were stained with haematoxylin and eosin (H&E stain) and  
142 scored (category 0 - 5) according to Adams and Nowak (2001) [24]. Briefly, the number of  
143 lesions occurring dorsally, medially and ventrally in the gill filaments were noted, along with  
144 size of lesion, the degree of pathological severity and pathological changes, with a score of 0  
145 (none), 1 (light), 2 (mild), 3 (moderate), advanced (4), and 5 (severe).

### 146 2.3 RNA extraction and cDNA synthesis

147 Total RNA isolation from the gill samples was conducted using TRIzol, following the  
148 manufacturer's instructions (TRIzol® Reagent, Ambion®). Total RNA was dissolved in 50 –  
149 60  $\mu\text{l}$  diethylpyrocarbonate (DEPC)-treated water and concentration [ $\text{ng}/\mu\text{l}$ ] determined on a  
150 NanoDrop ND-1000 Spectrophotometer (PEQLAB GmbH, Germany). To assess the sample  
151 quality, the A260/A280 and A260/A230 ratios were checked to ensure that the RNA had an  
152 A260/A280 ratio of  $\sim 2.0$  and that the A260/A230 ratio was in the range of 1.8 – 2.2.

153 To guarantee constant and comparable amounts of RNA in the analyses, the concentration of  
154 treated RNA was set to approximately 1000 ng of total RNA per assay for the reverse  
155 transcription (RT), to reach a final concentration of approximately 50  $\text{ng}/\mu\text{l}$  of input total  
156 RNA. The RNA was treated with gDNA Wipeout Buffer (QuantiTect Reverse Transcription  
157 Kit, Qiagen) to remove genomic DNA (gDNA) contamination and incubated for 2 min at 42  
158  $^{\circ}\text{C}$ . Each RT was performed in a mix containing: 14  $\mu\text{l}$  RNA previously treated to eliminate  
159 gDNA, 1  $\mu\text{l}$  of reverse-transcription master mix (reverse transcriptase and RNase inhibitor), 4  
160  $\mu\text{l}$  of Quantiscript RT Buffer, 1  $\mu\text{l}$  of RT Primer Mix optimized blend of oligo-dT and  
161 random primers dissolved in water (QuantiTect Reverse Transcription Kit, Qiagen). The  
162 mixture was incubated at 42  $^{\circ}\text{C}$  for 30 min and afterwards the enzyme was inactivated at 95  
163  $^{\circ}\text{C}$  for 3 min. A negative cDNA control sample with DEPC-treated water (Invitrogen™,  
164 Carlsbad, USA) instead of reverse transcriptase was included to check for cDNA quality. The  
165 generated cDNA template was diluted 1:10 with DEPC-treated water and then stored at - 20  
166  $^{\circ}\text{C}$  until real time RT-PCR analysis.

### 167 2.4 Real time RT-PCR

168 Real time RT-PCR was carried out using a LightCycler® 480 (Roche Applied Science) in a  
169 20  $\mu\text{l}$  reaction using SYBR® Green I Nucleic Acid Gel Stain (Invitrogen™, Carlsbad, USA)  
170 and IMMOLASE™ DNA Polymerase (Bioline, UK). 4  $\mu\text{l}$  cDNA (corresponding to 20 ng of  
171 input total RNA) were used in each reaction to maintain data integrity for gene expression  
172 comparisons. The real time analysis program consisted of 1 cycle of denaturation (95  $^{\circ}\text{C}$  for

173 10 min), 40 cycles of amplification (95 °C for 30 s, 63 °C for 30 s, 72 °C for 20 s, 84 °C for 5  
174 s), followed by 95 °C for 5 s and 75 °C for 1 min. Program profiles differed for annealing  
175 temperature and time for elongation. At least one of each real time RT-PCR primer pair was  
176 designed to cross an exon-intron boundary to avoid amplification of gDNA (Table 1). Primer  
177 efficiency was tested using 10 fold serial dilutions of cDNA [25] from pooled RNA samples  
178 and calculated by the 'LightCycler® 480 software version 1.5.1.62' (Roche Applied Science)  
179 as  $E\% = 10^{(-1/s)}$ , where s is the slope generated from the Log dilution of cDNA plotted  
180 against Cp (cycle number of crossing point). A sample of genomic DNA from muscle of  
181 Atlantic salmon parr was used in each real time RT-PCR assay to confirm that no gDNA was  
182 amplified.

183 Each quantification was carried out in duplicate and a sample containing only DEPC-treated  
184 water instead of cDNA was used as a negative control. The expression level of the gene of  
185 interest (GOI) relative to that of the reference gene elongation factor-1 $\alpha$  (EF-1 $\alpha$ ) was  
186 calculated by the 'Relative expression software tool' (REST©) [25, 26]. Cytokines  
187 potentially involved in adaptive immunity and released by Th cells, and arginase as a marker  
188 of alternatively activated macrophages, were studied.

### 189 2.5 Correlation analyses between amoeba load and GOIs

190 *P. perurans* load in each sample was determined by analysing the amoeba 18S rRNA by real  
191 time RT-PCR, as it was reported previously that there is a linear relationship between the log  
192 of 18S rRNA copies derived from plasmid DNA containing a partial *N. perurans* 18S RNA  
193 gene and DNA extracted from increasing numbers of *N. perurans* trophozoites [27]. For *P.*  
194 *perurans* load the same cDNA samples were used as for the gene expression analysis. The  
195 association between the *P. perurans* load (18S rRNA) Cp values at two different  
196 concentrations was tested by a linear regression model (R software, software 3.0.1).  
197 Normality of the GOI and *P. perurans* load Cp values was tested with a Shapiro-Wilk's W-  
198 Test (R software, software 3.0.1), which found that the Cp data were not normally distributed  
199 ( $p > 0.05$ ,  $n = 5$ ) both for the GOI and the *P. perurans* load. Therefore, to test the correlation  
200 between the *P. perurans* load and gene expression Cp values, a non-parametric test  
201 (Spearman's rank correlation coefficient) was applied (GraphPad Prism® Software, version  
202 5.04) (Table 2).

## 203 2.6 *Immunohistochemistry*

204 Gill tissues from the first gill arch were snap frozen in liquid nitrogen and stored at - 80 °C.  
205 They were then embedded in Tissue-Tek® optimum cutting temperature (O.C.T.) compound  
206 (VWR Chemicals) and sectioned (10 µm) using a cryostat (Leica CM1850 UV; Leica  
207 Microsystems). The sections were mounted onto SuperFrost® UltraPlus (Menzel-Gläser)  
208 positively charged glass slides and dried overnight at room temperature. Slides were then  
209 stored at - 80 °C until antibody staining. The slides were thawed and the tissue fixed in 4%  
210 phosphate buffered formaldehyde for 15 min, and then washed with tap water. Staining was  
211 performed using a Leica Bond-Max autostainer (Leica Microsystems), using the Bond  
212 Polymer Refine Detection system. The main steps used in the detection system are: 1)  
213 incubation with hydrogen peroxide for 5 min; 2) application of the specific primary antibody  
214 for 15 min; 3) a post antibody treatment that prepares the tissue for penetration of the  
215 subsequent polymer reagent for 8 min; 4) incubation with the polymer reagent, which  
216 included the polymeric horseradish peroxidase (HRP) – secondary antibody conjugates that  
217 recognize both mouse and rabbit immunoglobulins - for 8 min; 5) 3,3'-diaminobenzidine  
218 (DAB) for 10 min; 6) haematoxylin counterstaining that allows the detection of cell nuclei for  
219 5 min. After the staining, samples were washed with tap water for 10 s, then incubated with  
220 70% EtOH for 30 s, 100% EtOH for 30 s, and then xylene (3 dips). Slides were finally  
221 covered using a Coverslip Leica CV5030 (Leica Microsystems). Gill tissues from negative  
222 control fish and fish in the two treatments (three fish each) were used for  
223 immunohistochemistry using an anti - salmonid IgM (4c10) monoclonal antibody (mAb),  
224 diluted 1:15 [28]. Consecutive sections from the same fish were used for H&E staining and  
225 for a negative control, with a different primary mAb against respiratory syncytial virus -  
226 clone 4.15 [29].

## 227 2.7 *Statistical analysis*

228 A Kruskal-Wallis one-way analysis of variance was used as a non-parametric test to compare  
229 the terminal pathology following infection with the two concentrations of trophozoites (500  
230 cells/l and 5000 cells/l), and Dunn's Multiple Comparison Test was applied to compare  
231 differences in the sum of ranks (GraphPad Prism® Software, version 5.04). A pairwise fixed  
232 reallocation randomization test (software REST©) was used to compare gene expression  
233 analysis. This method has the advantage of making no distributional assumption about the

234 data, is more flexible than non-parametric tests, does not suffer from a reduction in power  
235 relative to parametric tests, and is based on randomization tests [26].

### 236 **3 Results**

#### 237 *3.1 Histopathology*

238 Pathological changes in the gills (e.g. hyperplasia) were scored as 0 - 5 for each fish,  
239 according to the degree of severity. The negative control (gills from fish exposed to culture  
240 media containing culture bacteria) had a gill score of 1 across all five fish. A Kruskal-Wallis  
241 one-way analysis of variance was used to compare the difference in the sum of ranks among  
242 all the treatments. Medians between the negative control (culture media) and gills, from fish  
243 exposed to the higher concentration of trophozoites (5000 cells/l), differed significantly with  
244 a p-value of 0.0031 (n = 5), based on a Gaussian approximation (Fig. 2). Comparisons  
245 between the negative control and gills from fish exposed to the lower concentration of  
246 trophozoites (500 cells/l), and between gills from fish given the two concentrations of *P.*  
247 *perurans* trophozoites (500 cells/l and 5000 cells/l), did not reveal any significant differences  
248 ( $p > 0.05$ , n = 5).

#### 249 *3.2 Gene expression analysis*

250 Some of the signature cytokines associated with Th1 and Th17 effector cells were found to be  
251 significantly down regulated in the gene expression analysis, mostly in samples from fish  
252 given the higher concentration of amoebae (5000 cells/l) (Figs. 3 and 4). For example, IFN- $\gamma$   
253 ( $p < 0.05$ , n = 5) and one of the isoforms of TNF- $\alpha$  (TNF- $\alpha_3$ ,  $p < 0.001$ , n = 5; [30]), related  
254 to the Th1 effector cells, and IL-17A/F1b ( $p < 0.01$ , n = 5) [31, 32], IL-17D ( $p < 0.001$ , n = 5)  
255 and IL-22 ( $p < 0.01$ , n = 5) [33] associated with Th17 effector cells, were all significantly  
256 down regulated in comparison to the controls. Transforming growth factor (TGF)- $\beta$ 1 and IL-  
257 10, regulatory cytokines highly produced by Treg cells, also showed a significant down  
258 regulation in comparison to the controls, for both isoforms, in the case of IL-10 in gills from  
259 fish given the higher concentration of trophozoites (IL-10A with a p-value  $< 0.01$ , IL-10B  
260 with a p-value  $< 0.05$ , n = 5) [34]. Only one isoform of TGF- $\beta$ 1 (TGF- $\beta$ 1B, [35]) was  
261 significantly down regulated, but at both concentrations of trophozoites (500 cells/l with a p-  
262 value  $< 0.01$ , and 5000 cells/l with a p-value  $< 0.001$ , n = 5) (Fig. 5). In the case of the two  
263 isoforms of IL-4/13 (IL-4/13A, IL-4/13B1) [36, 37], that are potentially involved in Th2  
264 effector cell responses, both were found to be significantly up regulated ( $p < 0.001$ , n = 5) in

265 comparison to the control in gills from fish given the higher concentration of trophozoites,  
266 with IL-4/13A also affected in gills exposed to the lower concentration (Fig. 6). Lastly, gene  
267 expression analysis of the enzyme arginase, induced by macrophages activated by Th2-type  
268 cytokines during the so-called ‘alternative macrophage activation’ (alternative M2  
269 activation), was studied and revealed a significant down regulation ( $p < 0.01$ ,  $n = 5$ ) in gills  
270 exposed to the higher concentration of trophozoites in comparison to gills exposed to the  
271 culture media (Fig. 7).

### 272 3.3 Correlation analyses between *P. perurans* load and GOIs

273 A linear regression analysis was performed to estimate the relationship between the *P.*  
274 *perurans* load (18S rRNA) Cp values in gills exposed to the two different initial  
275 concentrations of the amoeba (500 cells/l and 5000 cells/l). As expected, it was found that the  
276 *P. perurans* load 18S rRNA (Cp values) was significantly different ( $p < 0.01$ ,  $n = 5$ ) between  
277 the gills from fish exposed to the two doses, being significantly higher at the higher dose  
278 (Fig. 8). The constancy of variance and normality of residuals were checked for the validation  
279 of the analysis with model-checking plots (data not shown).

280 Spearman’s rank correlation coefficient was used to test the correlation between the Cp  
281 values of GOI and the Cp values of *P. perurans* load in the gill samples (Table 2). A negative  
282 correlation coefficient was found for all the genes except for the two IL-4/13 isoforms and  
283 IL-17A/F2a that showed a fold change higher than the fold change of the negative control  
284 (culture media) gill samples. The strongest and most significant relationships were seen with  
285 the negative correlations for IFN- $\gamma$ , IL-17A/F1b, IL-22, and TGF- $\beta$ 1B (Table 2).

### 286 3.4 Immunohistochemistry

287 In order to examine possible downstream effects of the up regulation of IL-4/13, the presence  
288 of immunoglobulin-positive lymphocytes in gill tissue during the AGD infection was studied  
289 using a mAb to salmonid IgM (4c10) to detect IgM<sup>+</sup> B cells by immunohistochemistry. IgM<sup>+</sup>  
290 cells were not found in the hyperplastic lesion associated with AGD infection, and were  
291 detected only in association with putative blood capillaries. H&E stained slides confirmed the  
292 existence of the blood capillaries within the gill sections. Negative controls, using a different  
293 primary antibody, on a consecutive gill section for each fish, did not show a positive reaction,  
294 confirming the positive results seen using the anti-IgM mAb.

## 295 4 Discussion

296 An investigation of the immune response elicited in the interbranchial lymphoid tissue (ILT)  
297 can increase our understanding of the role of this tissue in adaptive immunity during late  
298 stage AGD infection. The ILT consists largely of T-cells embedded in a meshwork of  
299 epithelial cells [19], therefore different cytokines, potentially involved in the development of  
300 and secreted by different effector T cells of the CD4<sup>+</sup> lineage, have been screened by gene  
301 expression analysis in this study.

302 Initially, following infection of fish with two different exposure concentrations of amoebae  
303 (500 cells/l and 5000 cells/l) for a period of 3 weeks, we assessed the pathological changes in  
304 the gills (gill score) and *P. perurans* load (18S rRNA) for each fish in the experiment.  
305 Histopathological changes in gill score showed significant differences between gills from the  
306 negative control (culture media) group and fish exposed to the higher concentration of  
307 trophozoites, whereas analysis of the *P. perurans* load by real time RT-PCR (18S rRNA)  
308 found a significant difference between Cp values of gill samples from fish exposed to an  
309 initial concentration of 500 cells/l versus 5000 cells/l (Fig. 8). The apparent lack of a precise  
310 association between gill pathology (gill score) and *P. perurans* load may indicate  
311 heterogeneity of both methods across different regions of the first gill arch, similar to that  
312 seen for the transcriptional response to AGD infection in gill tissue with lesions and without  
313 lesions [1]. To test the correlation between the Cp values of the GOI studied and the Cp  
314 values for *P. perurans* load in the gill samples, Spearman's rank correlation coefficient was  
315 used. Significant relationships were only seen with the negative correlations for IFN- $\gamma$ , IL-  
316 17A/F1b, IL-22 and TGF- $\beta$ 1B suggesting that results in gene expression profiles and the  
317 presence of *P. perurans* in infected gills are not always directly correlated (Table 2).

318 Gene expression profiles of signature cytokines produced by Th subsets (Th1, Th2, Th17,  
319 Treg) were screened in the ILT of Atlantic salmon exposed to the two different  
320 concentrations of amoebae, to assess their potential role in host defences against this parasite.  
321 The main function of Th1 cells is to activate macrophages and destroy intracellular microbes  
322 following phagocytosis. The principal signature cytokine of Th1 cells is IFN- $\gamma$  although TNF  
323 is also released after activation of Th1 cells. In this study, gene expression analysis showed  
324 that IFN- $\gamma$  and one of the isoforms of TNF- $\alpha$  (TNF- $\alpha$ 3) were significantly down regulated in  
325 comparison to gill tissue from the negative control when the samples were from fish exposed  
326 to the higher concentration of trophozoites (5000 cells/l). Two other salmon isoforms of  
327 TNF- $\alpha$  (TNF- $\alpha$ 1, TNF- $\alpha$ 2) were not significantly down regulated, similar to previous findings

328 at an early stage of AGD infection in Atlantic salmon [12]. Differences in the expression of  
329 the TNF- $\alpha$  isoforms suggest that TNF- $\alpha$ 3 may have some unique functions and expression  
330 characteristics, as was also seen in a previous study where a differential expression and  
331 modulation of these paralogues was hypothesized as a subfunctionalisation that allows a fine-  
332 tuned gene regulation [30]. Th17 cells secrete IL-17 and IL-22 cytokines that mainly recruit  
333 neutrophils to the site of infection. IL-17 is a key cytokine produced by Th17 cells which is  
334 involved in the inflammatory and neutrophil response, and IL-22 is a IL-10 cytokine family  
335 member involved in different aspects of the immune response including its production by  
336 activated T cells with a role in downstream production of antimicrobial peptides and a  
337 promotion of barrier function and tissue repair at the level of epithelial cells. The expression  
338 of IL-17A/F1b, IL-17D and IL-22 were found to be significantly down regulated in  
339 comparison to the negative control also in gills from fish exposed to the higher concentration  
340 of trophozoites.

341 Treg cells produce IL-10 and TGF- $\beta$  that inhibit immune responses. Among the different and  
342 diverse roles that these cytokines have in the immune system, TGF- $\beta$  is involved in the  
343 inhibition of T cell proliferation and macrophage activation, and promotes the development  
344 of Th17 cells and tissue repair after a local immune and inflammatory reaction. IL-10 inhibits  
345 the production of IL-12, suppressing the secretion of IFN- $\gamma$  and subsequent activation of  
346 innate and adaptive cell-mediated responses. Only one isoform of the two known salmonid  
347 TGF- $\beta$ 1 genes (TGF- $\beta$ 1B) was found to be significantly down regulated in comparison to the  
348 negative control, at both concentrations of trophozoites, but both isoforms of IL-10 were  
349 found to be significantly down regulated in gills from fish exposed to the higher  
350 concentration of trophozoites. That TGF- $\beta$ 1B is more responsive to a range of stimulants has  
351 been seen previously, as in trout head kidney (HK) macrophages exposed to bacterial and  
352 viral pathogen associated molecular patterns (PAMPs), proinflammatory cytokines, mitogens  
353 and pathway activators where highly elevated levels of TGF- $\beta$ 1B are seen but TGF- $\beta$ 1A is  
354 unchanged [35]. Down regulation of the Th17 pathway could be potentially explained by the  
355 suppression of TGF- $\beta$ 1B expression. Both down regulation of TGF-  $\beta$ 1B and IL-10 could be  
356 related to an imbalance of the immune system resulting in a severe inflammatory reaction in  
357 the gills, caused by the presence of the amoeba, which limits tissue repair mechanisms [38].  
358 Similar imbalances have been described during chronic inflammatory conditions in mammals  
359 [38].

360 Overall, cytokines related to the Th1, Th17 and Treg pathways were found to be significantly  
361 down regulated, mostly in gill samples from fish exposed to the higher concentration of

362 amoebae (Figs. 3-5). In contrast, IL-4/13A and IL-4/13B1, believed to be related to the Th2  
363 pathway, were found to be significantly up regulated (Fig. 6). More variation in gene  
364 expression among individuals (as seen by the standard error bars) was found at the lower  
365 infection dose, suggesting a higher variability in infection/responsiveness when using lower  
366 doses of trophozoites. Th2-mediated immune responses are induced by extracellular parasites  
367 [39] and the secretion of IL-4 can be involved either in inducing an alternative pathway of  
368 macrophage activation or in the production of antibodies. In order to test the potential effects  
369 of the up regulation of IL-4/13, gene expression analysis of the enzyme arginase that is  
370 induced in macrophages by alternative (M2) activation and immunohistochemistry (IHC)  
371 analysis that investigated the role of immunoglobulin-positive lymphocytes in AGD affected  
372 gill tissue were carried out. Gene expression analysis of arginase revealed a significant down  
373 regulation in comparison to the negative control in gill tissues from fish expose to the higher  
374 concentration of trophozoites (Fig. 7). This suggests that the up regulation of IL-4/13 is not  
375 related to a downstream activation of macrophages. The IHC analysis revealed that IgM  
376 positive cells were not found in hyperplastic lesions associated with AGD infection (Fig. 9),  
377 and were only detected in blood vessels/capillaries in the sections. Hence there was no  
378 evidence for proliferation of IgM positive cells or a local IgM humoral response to the  
379 parasite where the pathology is present, although we cannot exclude a role for IgT at the  
380 present time. Similar findings in gene expression analysis have been found in skin of rainbow  
381 trout *Oncorhynchus mykiss* (Walbaum, 1792) infected with the parasitic flagellate  
382 *Ichthyobodo necator* (Henneguy, 1883), where the up regulation of IL-4/13A and IL-10  
383 genes were found as well as the transcription factor GATA3 that is connected to the  
384 proliferation of B cells. It was suggested that a partial shift towards a Th2 response was  
385 occurring with the *I. necator* infection [40]. Interestingly, *P. perurans* possesses one or more  
386 intracellular perinuclear bodies, known as ‘parasomes’ [41]. These ‘parasomes’ are  
387 eukaryotic endosymbionts that are described as *Perkinsela amoebae* (Hollande, 1980) - like  
388 organisms and seem to be related phylogenetically to flagellated, parasitic marine protozoans  
389 (i.e. *Ichthyobodo* spp.) [2, 41, 42]. Thus, the similar findings in relation to the up regulation  
390 of the IL-4/13A in skin of rainbow trout infected with *I. necator* and the two IL-4/13  
391 isoforms shown in this study may reflect the phylogenetic relatedness of *I. necator* to the  
392 eukaryotic endosymbionts present in *P. perurans*, perhaps suggesting that the eukaryotic  
393 endosymbionts might have a role in the pathogenicity seen during AGD.  
394 In humans, Th2-driven responses are characterized by the activation of humoral immunity  
395 and the production of IgE, and in the majority of worm infections this results in the

396 generation of a Th2-mediated response that directs the immune system away from a Th1  
397 inflammatory response [39]. Furthermore, it is known that the balance between the Th2 cells  
398 and Treg cells is important during allergic diseases. During human allergic disease, effector  
399 Th2 cells produce IL-4, IL-5, IL-9, and IL-13 and these cytokines induce the production of  
400 allergen-specific IgE by B cells, development and recruitment of eosinophils, and production  
401 of mucus [43]. Treg cells directly or indirectly suppress effector cells of allergic  
402 inflammation, such as mast cells, basophils, and eosinophils, and contribute to remodelling in  
403 asthma and atopic dermatitis [43]. Increased levels of IL-10 and TGF- $\beta$  produced by Treg  
404 cells can suppress IgE production and can be important for control of allergic inflammation.  
405 Down regulation of IL-10 and TGF- $\beta$ , as seen in this study, might be a limiting factor for the  
406 development of a healthy immune response in the case of an allergic reaction to *P. perurans*  
407 occurring during AGD infection. However, in the present study, the up regulation of IL-4/13  
408 was not associated with either up regulation of arginase or an increase in IgM positive cells in  
409 the hyperplastic lesions, and it may either represent an immune evasion strategy used by the  
410 parasite to avoid cell-mediated killing mechanisms, or an allergic reaction caused by the  
411 parasite itself.

412

413 In conclusion, signature cytokines related to Th1, Th17 and Treg pathways were found to be  
414 significantly down regulated, mainly in gill samples from fish exposed to the higher dose of  
415 amoebae. In contrast, IL-4/13 expression, potentially involved in the Th2 pathway, was found  
416 to be significantly up regulated in gills from both trophozoite exposed groups. The lack of  
417 evidence for activation of the alternative macrophage pathway and the absence of IgM  
418 positive cells in the hyperplastic lesions associated with AGD infection may suggest that  
419 either an immune evasion strategy, similar to the responses driven by helminthic parasites to  
420 avoid cell-mediated killing mechanisms, or an allergic mechanisms caused by the parasite, is  
421 occurring in AGD infected fish.

422 **Ethics statement:** All handling of fish was conducted in accordance with the Animals  
423 (Scientific Procedures) Act 1986 and all proposed experiments were first subject to detailed  
424 statistical review to ensure that a minimum number of fish was used, which would allow  
425 statistically meaningful results to be obtained.

426 **Acknowledgments**

427 This work was supported financially by the Marine Collaboration Research Forum (MarCRF)  
428 which is a collaboration between the University of Aberdeen and Marine Scotland Science,  
429 Marine Laboratory (MSS). Thanks go Dr. David Bruno (MSS) and Patricia Noguera (MSS)  
430 for the assessment of the gill score AGD pathology; Dr. Malcolm Hall (MSS) for statistical  
431 consultancy; Louise Feehan (MSS), Ben Williamson (MSS) and Mark Paterson (MSS) for  
432 the management of the aquarium and the fish care; Mark Fordyce (MSS) for the H&E stain  
433 and scan of the slides; Dr. Ayham Alnabulsi for providing the anti-Ig antibodies; the  
434 histology facility at the Institute of Medical Sciences, University of Aberdeen; Carola Dehler  
435 for providing the Atlantic salmon DNA muscle samples used for checking whether  
436 amplification of gDNA occurred.

437

438 **References**

- 439 [1] Pennacchi Y, Leef MJ, Crosbie PBB, Nowak BF, Bridle AR. Evidence of immune and  
440 inflammatory processes in the gills of AGD-affected Atlantic salmon, *Salmo salar* L.  
441 Fish & Shellfish Immunology 2014 2;36(2):563-70.
- 442 [2] Young ND, Crosbie PBB, Adams MB, Nowak BF, Morrison RN. *Neoparamoeba*  
443 *perurans* n. sp., an agent of amoebic gill disease of Atlantic salmon (*Salmo salar*).  
444 International Journal for Parasitology 2007;37(13):1469-81.
- 445 [3] Crosbie PBB, Bridle AR, Cadoret K, Nowak BF. In vitro cultured *Neoparamoeba*  
446 *perurans* causes amoebic gill disease in Atlantic salmon and fulfils Koch's postulates.  
447 International Journal for Parasitology 2012;42(5):511-5.
- 448 [4] Feehan CJ, Johnson-Mackinnon J, Scheibling RE, Lauzon-Guay J-, Simpson AGB.  
449 Validating the identity of *Paramoeba invadens*, the causative agent of recurrent mass  
450 mortality of sea urchins in Nova Scotia, Canada. Diseases of Aquatic Organisms  
451 2013;103(3):209-27.
- 452 [5] Santos MJ, Cavaleiro F, Campos P, Sousa A, Teixeira F, Martins M. Impact of amoeba  
453 and scuticociliatidia infections on the aquaculture European sea bass (*Dicentrarchus*  
454 *labrax* L.) in Portugal. Veterinary Parasitology 2010;171(1-2):15-21.
- 455 [6] Crosbie PBB, Ogawa K, Nakano D, Nowak BF. Amoebic gill disease in hatchery-reared  
456 ayu, *Plecoglossus altivelis* (Temminck & Schlegel), in Japan is caused by  
457 *Neoparamoeba perurans*. Journal of Fish Diseases 2010;33(5):455-8.
- 458 [7] Bermingham ML, Mulcahy MF. Environmental risk factors associated with amoebic gill  
459 disease in cultured salmon, *Salmo salar* L., smolts in Ireland. Journal of Fish Diseases  
460 2004 OCT 2004;27(10):555-71.
- 461 [8] Young ND, Dyková I, Snekvik K, Nowak BF, Morrison RN. *Neoparamoeba perurans* is  
462 a cosmopolitan aetiological agent of amoebic gill disease. Diseases of Aquatic  
463 Organisms 2008;78(3):217-23.
- 464 [9] Steinum T, Kvellestad A, Rønneberg LB, Nilsen H, Asheim A, Fjell K, Nygård SMR,  
465 Olsen AB, Dale OB. First cases of amoebic gill disease (AGD) in Norwegian seawater  
466 farmed Atlantic salmon, *Salmo salar* L., and phylogeny of the causative amoeba using  
467 18S cDNA sequences. Journal of Fish Diseases 2008;31(3):205-14.
- 468 [10] Bustos PA, Young ND, Rozas MA, Bohle HM, Ildefonso RS, Morrison RN, Nowak BF.  
469 Amoebic gill disease (AGD) in Atlantic salmon (*Salmo salar*) farmed in Chile.  
470 Aquaculture 2011;310(3-4):281-8.
- 471 [11] Mouton A, Crosbie P, Cadoret K, Nowak B. First record of amoebic gill disease caused  
472 by *Neoparamoeba perurans* in South Africa. Journal of Fish Diseases 2013;37:407-9.
- 473 [12] Morrison RN, Zou J, Secombes CJ, Scapigliati G, Adams MB, Nowak BF. Molecular  
474 cloning and expression analysis of tumour necrosis factor- $\alpha$  in amoebic gill disease

- 475 (AGD)-affected Atlantic salmon (*Salmo salar* L.). Fish and Shellfish Immunology  
476 2007;23(5):1015-31.
- 477 [13] Bridle AR, Morrison RN, Cupit Cunningham PM, Nowak BF. Quantitation of immune  
478 response gene expression and cellular localisation of interleukin-1 $\beta$  mRNA in Atlantic  
479 salmon, *Salmo salar* L., affected by amoebic gill disease (AGD). Veterinary  
480 Immunology and Immunopathology 2006;114(1-2):121-34.
- 481 [14] Morrison RN, Young ND, Nowak BF. Description of an Atlantic salmon (*Salmo salar*  
482 L.) type II interleukin-1 receptor cDNA and analysis of interleukin-1 receptor expression  
483 in amoebic gill disease-affected fish. Fish and Shellfish Immunology 2012;32(6):1185-  
484 90.
- 485 [15] Morrison RN, Cooper GA, Koop BF, Rise ML, Bridle AR, Adams MB, Nowak BF.  
486 Transcriptome profiling the gills of amoebic gill disease (AGD)-affected Atlantic salmon  
487 (*Salmo salar* L.): A role for tumor suppressor p53 in AGD pathogenesis? Physiological  
488 Genomics 2006;26(1):15-34.
- 489 [16] Young ND, Cooper GA, Nowak BF, Koop BF, Morrison RN. Coordinated down-  
490 regulation of the antigen processing machinery in the gills of amoebic gill disease-  
491 affected Atlantic salmon (*Salmo salar* L.). Molecular Immunology 2008;45(9):2581-97.
- 492 [17] Morrison RN, Koppang EO, Hordvik I, Nowak BF. MHC class II<sup>+</sup> cells in the gills of  
493 Atlantic salmon (*Salmo salar* L.) affected by amoebic gill disease. Veterinary  
494 Immunology and Immunopathology 2006;109(3-4):297-303.
- 495 [18] Haugarvoll E, Bjerås I, Nowak BF, Hordvik I, Koppang EO. Identification and  
496 characterization of a novel intraepithelial lymphoid tissue in the gills of Atlantic salmon.  
497 Journal of Anatomy 2008;213(2):202-9.
- 498 [19] Koppang EO, Fischer U, Moore L, Tranulis MA, Dijkstra JM, Köllner B, Aune L, Jirillo  
499 E, Hordvik I. Salmonid T cells assemble in the thymus, spleen and in novel  
500 interbranchial lymphoid tissue. Journal of Anatomy 2010;217(6):728-39.
- 501 [20] Salinas I, Zhang Y-, Sunyer JO. Mucosal immunoglobulins and B cells of teleost fish.  
502 Developmental and Comparative Immunology 2011;35(12):1346-65.
- 503 [21] Austbø L, Aas IB, König M, Weli SC, Syed M, Falk K, Koppang EO. Transcriptional  
504 response of immune genes in gills and the interbranchial lymphoid tissue of Atlantic  
505 salmon challenged with infectious salmon anaemia virus. Developmental & Comparative  
506 Immunology 2014 7;45(1):107-14.
- 507 [22] Aas IB, Austbø L, König M, Syed M, Falk K, Hordvik I, Koppang EO. Transcriptional  
508 characterization of the T cell population within the salmonid interbranchial lymphoid  
509 tissue. Journal of Immunology 2014;193(7):3463-9.
- 510 [23] Norte Dos Santos CC, Adams MB, Leef MJ, Nowak BF. Changes in the interbranchial  
511 lymphoid tissue of Atlantic salmon (*Salmo salar*) affected by amoebic gill disease. Fish  
512 & Shellfish Immunology 2014 2014-Dec;41(2):600-7.

- 513 [24] Adams MB, Nowak BF. Distribution and structure of lesions in the gills of Atlantic  
514 salmon, *Salmo salar* L., affected with amoebic gill disease. *Journal of Fish Diseases*  
515 2001;24(9):535-42.
- 516 [25] Pfaffl MW. A new mathematical model for relative quantification in real-time RT-PCR.  
517 *Nucleic Acids Research* 2001 MAY 1 2001;29(9):e45.
- 518 [26] Pfaffl MW, Horgan GW, Dempfle L. Relative expression software tool (REST) for  
519 group-wise comparison and statistical analysis of relative expression results in real-time  
520 PCR. *Nucleic Acids Research* 2002;30(9).
- 521 [27] Bridle AR, Crosbie PBB, Cadoret K, Nowak BF. Rapid detection and quantification of  
522 *Neoparamoeba perurans* in the marine environment. *Aquaculture* 2010;309(1-4):56-61.
- 523 [28] Thuvander A, Fossum C, Lorenzen N. Monoclonal antibodies to salmonid  
524 immunoglobulin: Characterization and applicability in immunoassays. *Developmental*  
525 *and Comparative Immunology* 1990;14(4):415-23.
- 526 [29] Gimenez HB, Cash P, Melvin WT. Monoclonal antibodies to human respiratory  
527 syncytial virus and their use in comparison of different virus isolates. *Journal of General*  
528 *Virology* 1984;65(5):963-71.
- 529 [30] Hong S, Li R, Xu Q, Secombes CJ, Wang T. Two types of TNF- $\alpha$  exist in teleost fish:  
530 Phylogeny, expression, and bioactivity analysis of type-II TNF- $\alpha$ 3 in rainbow trout  
531 *Oncorhynchus mykiss*. *Journal of Immunology* 2013;191(12):5959-72.
- 532 [31] Monte MM, Wang T, Holland JW, Zou J, Secombes CJ. Cloning and characterization of  
533 rainbow trout interleukin-17A/F2 (IL-17A/F2) and IL-17 receptor  $\alpha$ : Expression during  
534 infection and bioactivity of recombinant IL-17A/F2. *Infection and Immunity*  
535 2013;81(1):340-53.
- 536 [32] Wang T, Jiang Y, Wang A, Husain M, Xu Q, Secombes CJ. Identification of the  
537 salmonid IL-17A/F1a/b, IL-17A/F2b, IL-17A/F3 and IL-17N genes and analysis of their  
538 expression following in vitro stimulation and infection. *Immunogenetics* 2015;in press.
- 539 [33] Monte MM, Zou J, Wang T, Carrington A, Secombes CJ. Cloning, expression analysis  
540 and bioactivity studies of rainbow trout (*Oncorhynchus mykiss*) interleukin-22. *Cytokine*  
541 2011;55(1):62-73.
- 542 [34] Harun NO, Wang T, Secombes CJ. Gene expression profiling in naïve and vaccinated  
543 rainbow trout after *Yersinia ruckeri* infection: Insights into the mechanisms of protection  
544 seen in vaccinated fish. *Vaccine* 2011;29(26):4388-99.
- 545 [35] Maehr T, Costa MM, González Vecino JL, Wadsworth S, Martin SAM, Wang T,  
546 Secombes CJ. Transforming growth factor- $\beta$ 1b: A second TGF- $\beta$ 1 paralogue in the  
547 rainbow trout (*Oncorhynchus mykiss*) that has a lower constitutive expression but is  
548 more responsive to immune stimulation. *Fish and Shellfish Immunology*  
549 2013;34(2):420-32.

- 550 [36] Takizawa F, Koppang EO, Ohtani M, Nakanishi T, Hashimoto K, Fischer U, Dijkstra  
551 JM. Constitutive high expression of interleukin-4/13A and GATA-3 in gill and skin of  
552 salmonid fishes suggests that these tissues form Th2-skewed immune environments.  
553 *Molecular Immunology* 2011 7;48(12–13):1360-8.
- 554 [37] Wang T, Secombes CJ. Molecular and functional characterisation of immune genes in  
555 salmonids. 2013;Acc. No. HG794522.
- 556 [38] Asadullah K, Sterry W, Volk HD. Interleukin-10 therapy - review of a new approach.  
557 *Pharmacological Reviews* 2003;55(2):241-69.
- 558 [39] Williams AE. *Immunology: Mucosal and body surface defences*. First ed. Oxford, OX4  
559 2DQ,UK: John Wiley & Sons, Ltd.; 2012.
- 560 [40] Chettri JK, Kuhn JA, Jaafar RM, Kania PW, Moller OS, Buchmann K. Epidermal  
561 response of rainbow trout to *Ichthyobodo necator*: Immunohistochemical and gene  
562 expression studies indicate a Th1-/Th2-like switch. *Journal of Fish Diseases* 2014  
563 SEP;37(9):771-83.
- 564 [41] Dyková I, Fiala I, Pecková H. *Neoparamoeba* spp. and their eukaryotic endosymbionts  
565 similar to *Perkinsella amoebae* (Hollande, 1980): Coevolution demonstrated by SSU  
566 rRNA gene phylogenies. *European Journal of Protistology* 2008;44(4):269-77.
- 567 [42] Dyková I, Fiala I, Lom J, Lukeš J. *Perkinsiella amoebae*-like endosymbionts of  
568 *Neoparamoeba* spp., relatives of the kinetoplastid *Ichthyobodo*. *European Journal of*  
569 *Protistology* 2003;39(1):37-52.
- 570 [43] Akdis M, Blaser K, Akdis CA. T regulatory cells in allergy: Novel concepts in the  
571 pathogenesis, prevention, and treatment of allergic diseases. *Journal of Allergy and*  
572 *Clinical Immunology* 2005 11;116(5):961-8.
- 573
- 574

575 **Figure legends**

576 **Fig. 1.** Localization of the gill samples taken from the first gill arch for gene expression  
577 analysis, which included primarily the interbranchial lymphoid tissue (ILT) avoiding the gill  
578 arch and the end of the gill filaments (© Marine Scotland Science).

579 **Fig. 2.** Gill scores from 0 (no pathology) to 5 (greatest pathology) were used to assess the gill  
580 samples from the first gill arch. A Kruskal-Wallis one-way analysis of variance was used to  
581 compare the difference in the sum of ranks (GraphPad Prism® Software, version 5.04)  
582 between the three groups. Different letters indicate significantly differences, \*\* =  $p < 0.01$ ,  $n$   
583 = 5.

584 **Fig. 3.** Relative expression of Th1 pathway genes (mean + SEM) as determined using  
585 REST© 2009 (relative expression software tool). The fold change was calculated as the  
586 relative expression in comparison to gills from the negative control (culture media) fish,  
587 normalized to EF-1 $\alpha$ . \* =  $p < 0.05$ , \*\*\* =  $p < 0.001$ ,  $n = 5$ .

588 **Fig. 4.** Relative expression of Th17 genes (mean + SEM) as determined using REST© 2009  
589 (relative expression software tool). The fold change was calculated as the relative expression  
590 in comparison to gills from the negative control (culture media) fish, normalized to EF-1 $\alpha$ . \*\*  
591 =  $p < 0.01$ , \*\*\* =  $p < 0.001$ ,  $n = 5$ .

592 **Fig. 5.** Relative expression of Treg genes (mean + SEM) as determined using REST© 2009  
593 (relative expression software tool). The fold change was calculated as the relative expression  
594 in comparison to gills from the negative control (culture media) fish, normalized to EF-1 $\alpha$ . \*  
595 =  $p < 0.05$ , \*\* =  $p < 0.01$ , \*\*\* =  $p < 0.001$ ,  $n = 5$ .

596 **Fig. 6.** Relative expression of Th2 pathway genes (mean + SEM) as determined using  
597 REST© 2009 (relative expression software tool). The fold change was calculated as the  
598 relative expression in comparison to gills from the negative control (culture media) fish,  
599 normalized to EF-1 $\alpha$ . \*\*\* =  $p < 0.001$ ,  $n = 5$ .

600 **Fig. 7.** Relative expression of arginase (mean + SEM) as determined using REST© 2009  
601 (relative expression software tool). The fold change was calculated as the relative expression  
602 in comparison to gills from the negative control (culture media) fish, normalized to EF-1 $\alpha$ . \*\*  
603 =  $p < 0.01$ ,  $n = 5$ .

604 **Fig. 8.** Box and whisker plots showing the distribution of the Cp values with the 5 and 95  
605 percentiles. The relationship between the *P. perurans* load (18S rRNA) Cp values at the two  
606 different infection concentrations was tested with a linear regression model (\*\*  $p < 0.01$ ,  $n =$   
607 5). Note: higher Cp values correspond to a lower expression of the 18S rRNA in the sample;  
608 lower Cp values correspond to a higher expression of the 18S rRNA in the sample.

609 **Fig. 9.** A) H&E staining: arrow shows the location of a blood capillary; B) IHC staining with  
610 anti-IgM mAb: arrow shows the staining of antibody and IgM<sup>+</sup> B cells only in association  
611 with blood capillaries; C) IHC staining with a primary mAb to an unrelated antigen (negative  
612 control): arrow shows the position of the blood capillary; D) H&E staining: arrow shows the  
613 AGD pathology, with fusion of secondary lamellae; E) IHC staining with anti-IgM mAb:  
614 arrow shows the AGD pathology with no antibody staining; F) IHC staining with a primary  
615 mAb to an unrelated antigen (negative control): arrow shows the AGD pathology with fusion  
616 of the secondary lamellae.

617

**Table 1.** Primer sequences used for gene expression analysis (real time RT-PCR).

<b>Gene</b>		<b>Oligonucleotides (5' – 3')</b>
<b>EF-1<math>\alpha</math></b>	Forward	CAAGGATATCCGTCGTGGCA
	Reverse	ACAGCGAAACGACCAAGAGG <sup>*</sup>
<b>IFN-<math>\gamma</math></b>	Forward	GATGGGCTGGATGACTTTAGGATG
	Reverse	CCTCCGCTCACTGTCCTCAA
<b>TNF-<math>\alpha</math>1</b>	Forward	ACTGGCAACGATGCAGGACAA
	Reverse	GCGGTAAGATTAGGATTGTATTCACCCTCT
<b>TNF-<math>\alpha</math>2</b>	Forward	ACTGGCAACGATGCAGGATGG
	Reverse	GCGGTAAGATTAGGATTGTATTCACCCTCT
<b>TNF-<math>\alpha</math>3</b>	Forward	CACGGCAAGAAACAAGATCCCA
	Reverse	GATCCACTGGGGTTGTATTCACCTTCTA
<b>IL-4/13A</b>	Forward	ACCACCACAAAGTGCAAGGAGTTCT
	Reverse	CACCTGGTCTTGGCTCTTACAAC
<b>IL-4/13B2</b>	Forward	GAGACTCATCTATTGCGTATGATCATCG
	Reverse	TGCAGTTGGTTGGATGAAACTTATTGTA
<b>IL-17A/F1b</b>	Forward	ACACACGGACCACACTCCAGAC
	Reverse	GCGTCGATCGTCATAGGTAGTGTTGTA
<b>IL-17A/F2a</b>	Forward	ACCCTGGACCTGGAAAACCAC
	Reverse	GCTGAAGTGTAGAGTACCACGACCTG
<b>IL-17A/F3</b>	Forward	CTGGTGCTGGGTCTGATCATGT
	Reverse	GGTTCATCGTATGTGTGCTGTATG
<b>IL-17C2</b>	Forward	CGAAACCGGTACCAGACAGATGT
	Reverse	CCTCCACGCTATCGATGCTGTA
<b>IL-17D</b>	Forward	AGAAATCCTCGAGCAGATGTTTGG
	Reverse	GGGTCGTGGGAGATCCTGTATG
<b>IL-22</b>	Forward	GAAGGAACACGGCTGTGCTATTAAC
	Reverse	GATCTAGGCGTGCACACAGAAGTC
<b>TGF-<math>\beta</math>1A</b>	Forward	CTCACATTTTACTGATGTCACTTCCTGT
	Reverse	GGACAACCTGCTCCACCTTGTG
<b>TGF-<math>\beta</math>1B</b>	Forward	CATGTCCATCCCCAGAACT
	Reverse	GGACAACCTGTTCCACCTTGTGTT
<b>IL-10A</b>	Forward	GGATTCTACACCACTTGAAGAGCCC
	Reverse	GTCGTTGTTGTTCTGTGTTCTGTTGT
<b>IL-10B</b>	Forward	GGGATTCTAGACCACATCAAGAGTCC
	Reverse	GGGATTCTAGACCACATCAAGAGTCC
<b>Arginase</b>	Forward	CATGTCCTACCTCATCCACGAGC
	Reverse	GATGGGCTTCTTCACCTTTGAGAA

**Table 2.** Correlation coefficients between the Cp values of the gene of interest (GOI) and the Cp values of amoeba load (18S rRNA) in gill samples. Data were analysed using Spearman's rank order correlation (n = 10).

<b>Gene</b>	<b>Correlation coefficient</b>	<b>P-value</b>
<b>IFN-<math>\gamma</math></b>	- 0.6727	0.0390
<b>TNF-<math>\alpha</math>1</b>	- 0.4012	0.2475
<b>TNF-<math>\alpha</math>2</b>	- 0.1273	0.7330
<b>TNF-<math>\alpha</math>3</b>	- 0.4303	0.2182
<b>IL-4/13A</b>	0.4424	0.2044
<b>IL-4/13B2</b>	0.5758	0.0883
<b>IL-17A/F1b</b>	- 0.6727	0.0390
<b>IL-17A/F2a</b>	0.5758	0.0883
<b>IL-17A/F3</b>	- 0.0667	0.8651
<b>IL-17C2</b>	- 0.5515	0.1049
<b>IL-17D</b>	- 0.5879	0.0806
<b>IL-22</b>	- 0.7697	0.0126
<b>TGF-<math>\beta</math>1A</b>	- 0.0303	0.9460
<b>TGF-<math>\beta</math>1B</b>	- 0.8667	0.0022
<b>IL-10A</b>	- 0.2485	0.4918
<b>IL-10B</b>	- 0.1394	0.7072
<b>Arginase</b>	- 0.6242	0.0603

Fig. 1:

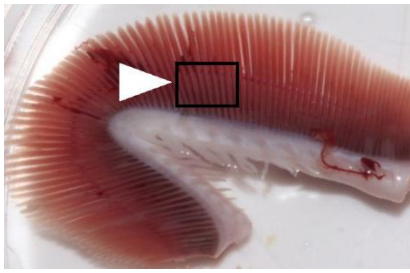


Fig. 2:

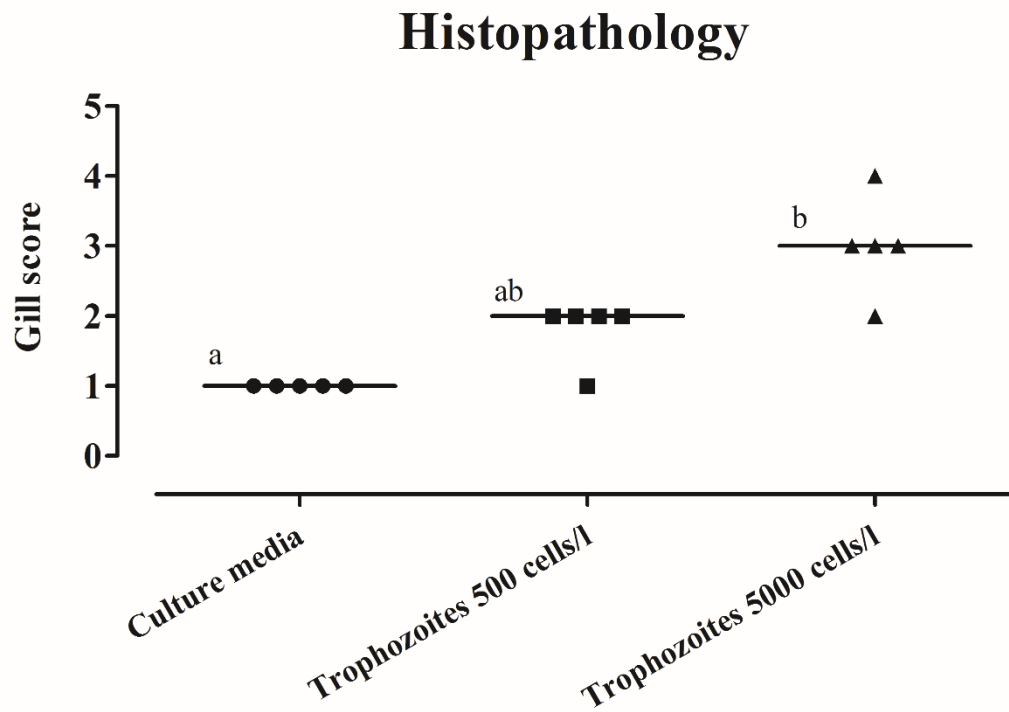


Fig. 3:

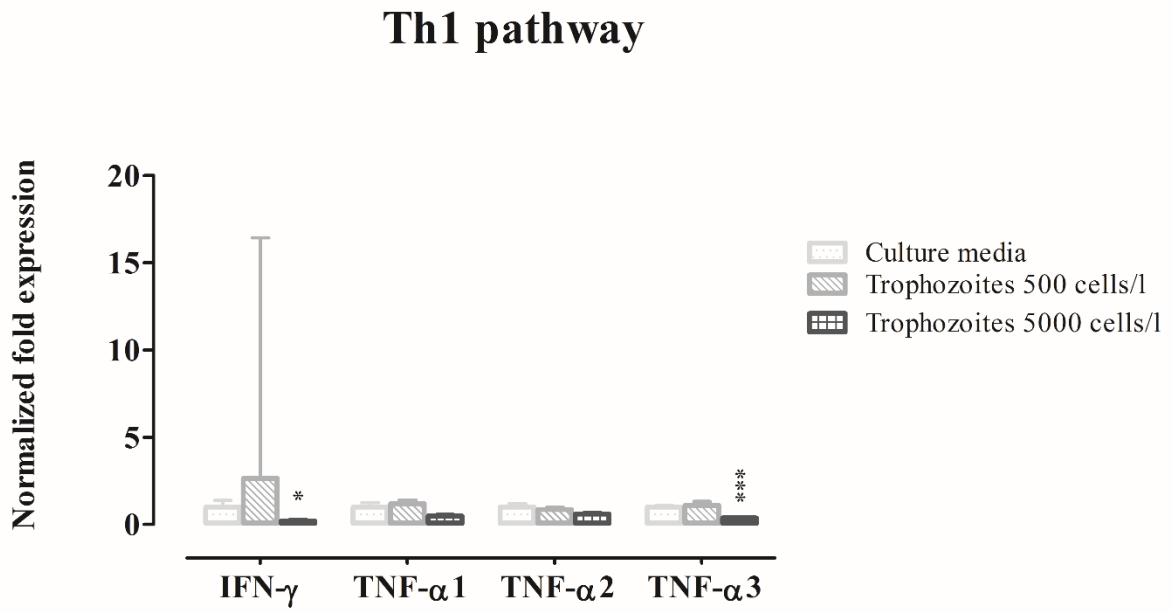


Fig. 4:

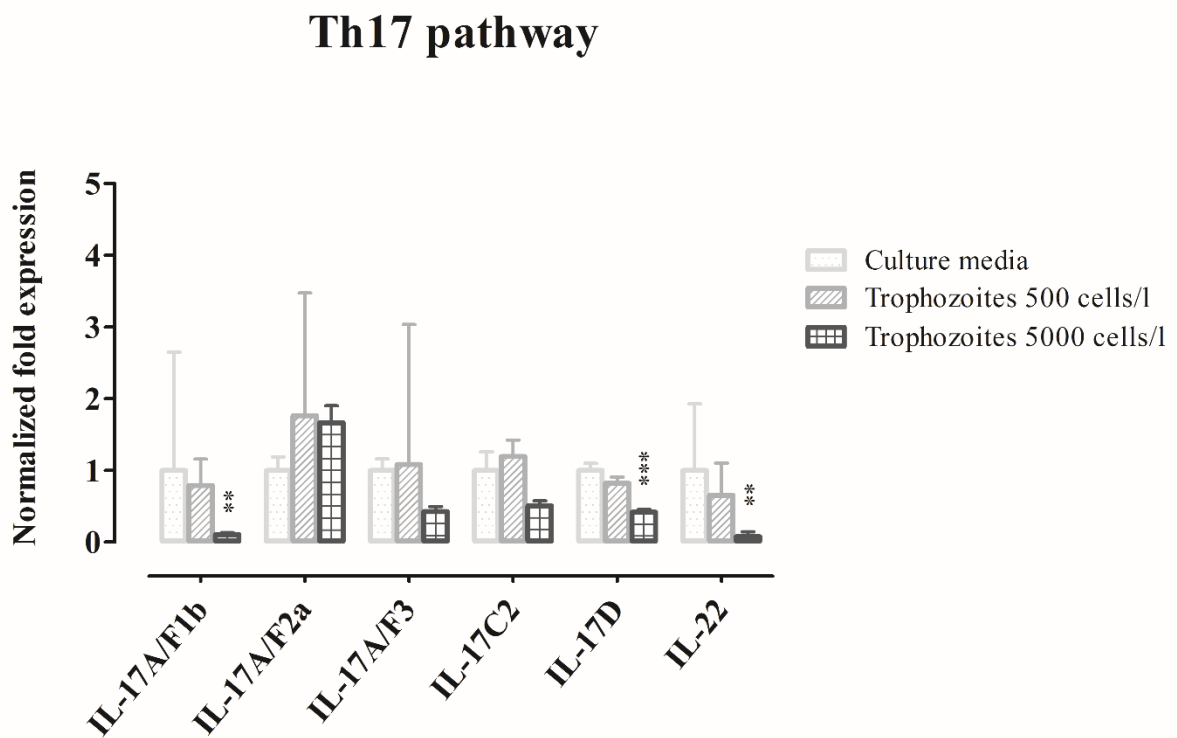


Fig. 5:

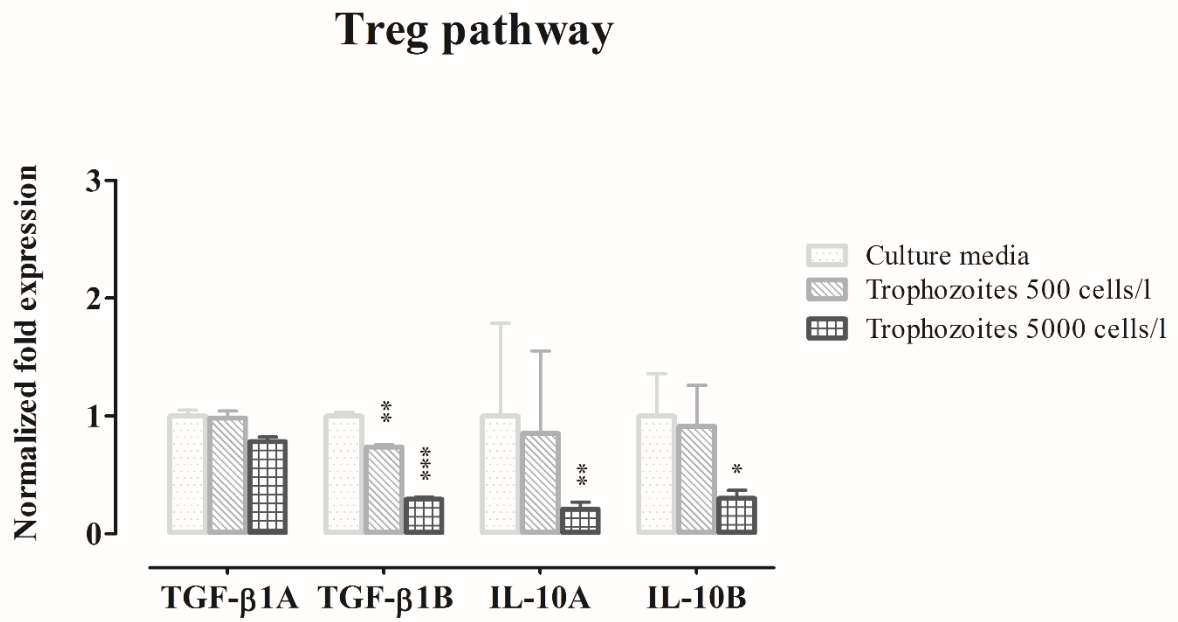


Fig. 6:

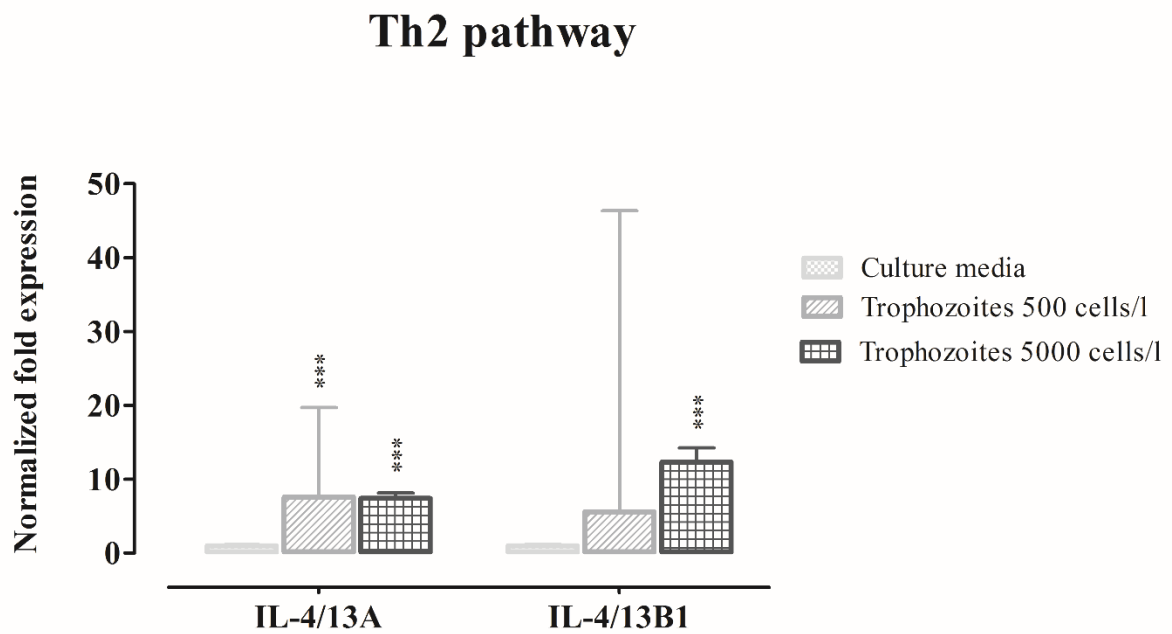


Fig. 7:

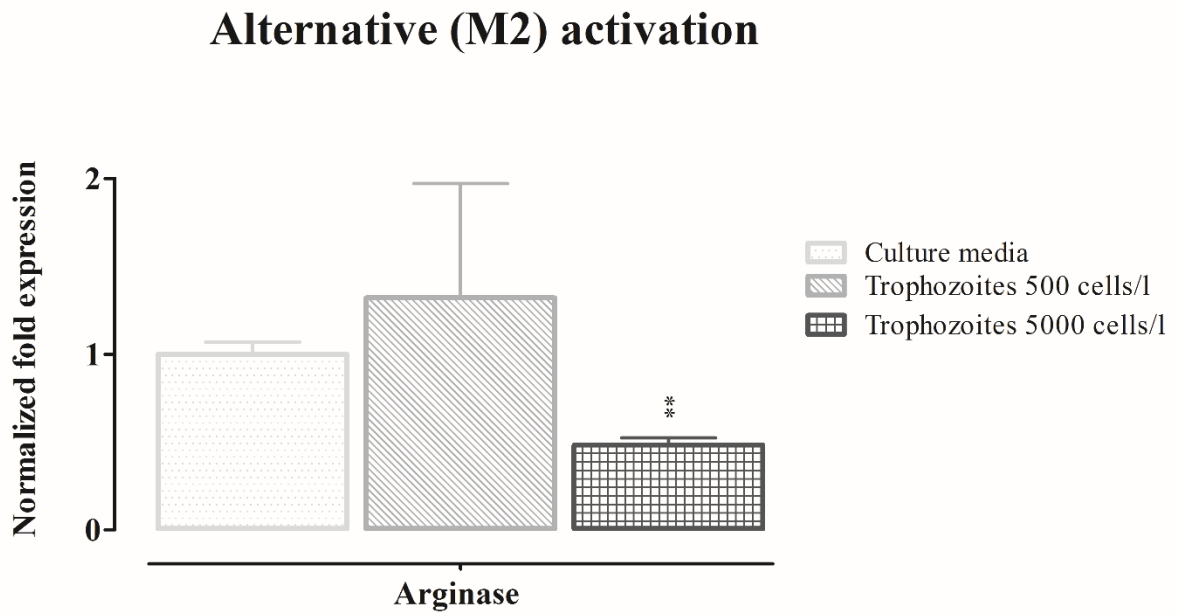
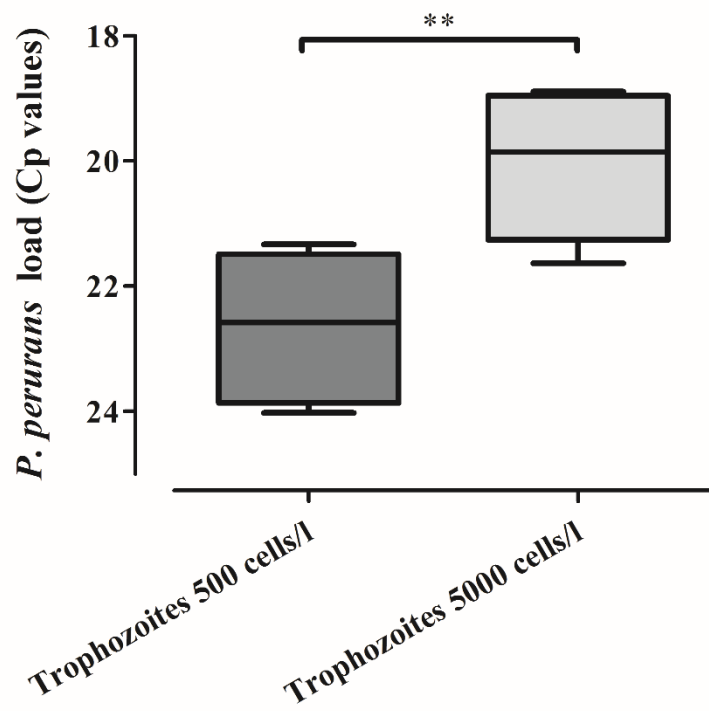


Fig. 8:



**Fig. 9:**

